Hum Genet (2003) 112 : 334–342
DOI 10.1007/s00439-003-0907-7

ORIGINAL INVESTIGATION

Michael Goldberg · Michelle Wei · Luwa Yuan
Vundavalli V. Murty · Benjamin Tycko

Biallelic expression of *HRAS* and *MUCDHL* in human and mouse

Received: 20 June 2002 / Accepted: 13 December 2002 / Published online: 14 February 2003

Abstract At least eight genes clustered in 1 Mb of DNA on human chromosome (Chr) 11p15.5 are subject to parental imprinting, with monoallelic expression in one or more tissues. Orthologues of these genes show conserved linkage and imprinting on distal Chr 7 of mice. The extended imprinted region has a bipartite structure, with at least two differentially methylated DNA elements (DMRs) controlling the imprinting of two sub-domains. We previously described three biallelically expressed genes (*MRPL23*, *2G7* and *TNNT3*) in 100 kb of DNA immediately downstream of the imprinted *H19* gene, suggesting that *H19* marks one border of the imprinted region. Here we extend this analysis to two additional downstream genes, *HRAS* and *MUCDHL* (mu-protocadherin). We find that these genes are biallelically expressed in multiple fetal and adult tissues, both in humans and in mice. The mouse orthologue of a third gene, *DUSP8*, located between *H19* and *MUCDHL*, is also expressed biallelically. The DMR immediately upstream of *H19* frequently shows a net gain of methylation in Wilms tumors, either via Chr 11p15.5 loss of heterozygosity (LOH) or loss of imprinting (LOI), but changes in methylation in CpG-rich sequences upstream and within the *MUCDHL* gene are rare in these tumors and do not correlate with LOH or LOI. These findings are further evidence for a border of the imprinted region immediately downstream of *H19*, and the data allow the construction of an imprinting map that includes more than 20 genes, distributed over 3 Mb of DNA on Chr 11p15.5.

M. Goldberg
Department of Pediatrics, College of Physicians and Surgeons, Columbia University,
630 West 168th Street, New York, NY, 10032, USA

M. Wei · L. Yuan · V. V. Murty · B. Tycko (✉)
Institute for Cancer Genetics,
College of Physicians and Surgeons, Columbia University,
630 West 168th Street, New York, NY, 10032, USA
Tel.: +1-212-8515280, Fax: +1-212-8515284,
e-mail: bt12@columbia.edu

V. V. Murty · B. Tycko
Department of Pathology, College of Physicians and Surgeons, Columbia University,
630 West 168th Street, New York, NY, 10032, USA

Introduction

Parental imprinting causes monoallelic expression of a small subset of mammalian genes. This has a number of consequences, including non-Mendelian inheritance of neurodevelopmental disorders, typified by Prader-Willi and Angelman syndromes, and of the preneoplastic overgrowth disorder, Beckwith-Wiedemann syndrome (Maher and Reik 2000; Nicholls 2000). A role for abnormal functional imprinting of two genes, *H19* and *IGF2*, is also established in several types of pediatric cancers, including Wilms tumor (WT) (Tycko 2000). Consistent with these findings from human genetics, data from knockout mice have suggested a disproportionate involvement of imprinted genes in regulating growth and behavior (Tycko and Morison 2002).

A striking feature of imprinted genes is that they are often found clustered together in the genome. The largest imprinted regions are those on human chromosome (Chr) 11p15.5, the region associated with BWS and WT, and Chr 15q11-q13, the region associated with PWS and AS. Genes in these two regions show conserved linkage with genes on the distal and mid-portions, respectively, of mouse Chr 7. The overall imprinted region of human Chr 11p15.5/mouse distal Chr 7 has a bipartite structure, with two differentially methylated DNA elements (DMRs) (Brannan and Bartolomei 1999) controlling the imprinting of two 'sub-domains' (Feinberg 2000; Horike et al. 2000). Here we examine two genes mapping near this imprinted region, *HRAS* and *MUCDHL*, for allele-specific mRNA expression, and we assess DNA methylation of *MUCDHL*. We combine the data with previous information to generate an updated imprinting map of this region.

Materials and methods

Analysis of DNA methylation by Southern blotting

For Southern analysis, genomic DNAs (3 µg) from WTs, non-neoplastic kidney parenchyma adjacent to the WTs, and a normal fetal kidney were digested with *Rsa*I, *Rsa*I plus *Hpa*II, or *Rsa*I plus *Cfo*I, resolved in 1% agarose gels, and transferred to nylon membranes. The blots were hybridized with appropriate probes for CpG-rich regions, which were generated by PCR of genomic DNAs using the primers listed in Table 1, and labeled with ^{32}P-dCTP by random priming (Random primers DNA labeling system, Life Technologies, Gaithersburg, Md.). High stringency hybridizations were done at 42 °C in ExpressHyb solution (Clontech, Palo Alto, Calif.) and the blots were washed for 15 min at room temperature in 2×SSC/0.1% SDS and then for 1 h at 65 °C in 0.1× SSC/0.1% SDS.

Analysis of DNA methylation by bisulfite conversion and sequencing

The procedure for bisulfite-mediated conversion was similar to published protocols (Herman et al. 1996). Briefly, genomic DNA (5 µg in 60 µl of water) was first denatured by adding 2.5 µl of 5 N NaOH and incubating at 37 °C for 10 min. Hydroquinone (36 µl of a 10 mM solution) was added, followed by addition of sodium bisulfite (622 µl of a 3 M solution) and incubation at 50 °C for 16 h. The bisulfite-converted DNA was then purified using Centricon YM-30 spin columns (Millipore, Bedford, Mass.), with elution in 50 µl of water. The DNA was desulphonated in 0.3 N NaOH at room temperature for 5 min, and then precipitated by adding an equal volume of 10 M ammonium acetate, followed by two volumes of ice-cold ethanol. The pellet was washed in 70% ethanol, dried briefly and dissolved in 50 µl of water. Each subsequent PCR reaction utilized 2 µl of the resulting DNA solution. Primers for amplifying the *MUCDHL* intragenic CpG-rich region from the bisulfite-converted DNA were: (upstream) ATTTGAGTTTTTTGGTTGATTTT; (downstream) AATAACATTTATATTCTCCTCTA. PCR was done using a touchdown procedure with 11 cycles of denaturation at 94 °C for 30 s, annealing at 60 °C for 30 s, and extension at 72 °C for 30 s; followed by 33 cycles using an annealing temperature of 50 °C, with a final extension at 72 °C for 10 min. The PCR products were gel-isolated, ligated into the TA-cloning vector (Promega) and the resulting clones sequenced.

Reverse transcription-PCR (RT-PCR) and analysis of allele-specific mRNA expression

Oligo-dT-priming and MuLV reverse transcriptase (Superscript, Life Technologies) were used to generate single-stranded cDNAs from mouse and human tissues. These were amplified by PCR using gene-specific primers and annealing temperatures listed in Table 1. Cycling employed an initial denaturation at 94 °C for 4 min, followed by 32 cycles of denaturation at 94 °C for 1 min, annealing at the indicated temperature for 30 s and extension at 72 °C for 1 min, with a final extension at 72 °C for 7 min. For each gene of interest, the relative amounts of mRNA derived from each allele were measured by either single-strand conformation polymorphism (SSCP) (Orita et al. 1989) or RFLP analysis. For SSCP and RFLP, the gel-isolated PCR products were internally radiolabeled by six cycles of PCR in the presence of ^{32}P-dCTP. After dilution in SDS/EDTA (0.1%/10 mM) and denaturation for SSCP, or direct loading of non-denatured restriction enzyme-digested products for RFLP (Table 1), these were resolved on 8% (*Hras*, *Nttp1*) or 6% (*HRAS, MUCDHL*) non-denaturing polyacrylamide gels (300 V

Table 1 PCR primers, conditions and restriction digestion for analysis of genomic SNPs and allele-specific mRNA expression

Gene	Primer name	Sequence	Experiment	Annealing temp. (°C)	Method: Restriction enzyme[a]
MUCDHL	MUCDHL-FOR1	CGTCCTTGTCCACAAGCAC	RT-PCR	58	SSCP: *Ava*I or *Dde*I
	MUCDHL-FOR2	AGCCCCAAGGCTTTGACAAC	Genomic PCR		
	MUCDHL-REV	AGATGTAGGAGTCATCACCAC	Genomic, RT-PCR		
	MUCDHL-CpG-F	AGGAGCCAAGCCAGGGCAG	Internal CpG-rich region probe	61	NA
	MUCDHL-CpG-R	GGGTGGACAAGGCTCCGAG			
	SCT-CpG-F	CCGGAACTCCGGCCGCAG	CpG-island probe	61	NA
	SCT-CpG-R	GAGGCCAGGACAGAAGGAGGG			
HRAS	HRAS-FOR	TATAAGCTGGTGGTGGTGGGCG	RT-PCR	56	SSCP: no digestion
	HRAS-REV	CGGTATCCAGGATGTCCAACAGG			
H19	H19-FOR	AACACCTTAGGCTGGTGGGG	Genomic, RT-PCR	56	RFLP: *Rsa*I
	H19-REV	CTAGTCTGGAAGCTCCGACCGA			
Mucdhl	MuEX7-FOR	TGCTGCTGGCACGGGTAAG	Genomic PCR	56	NA
	MuEX7-REV	CCTGGACCTGGACCTCCTTTC			
	MuEX8-FOR	GTTCTTGTTGCCACTGAGTCCTTC	Genomic PCR	56	NA
	MuEX8-REV	GTTGCCATCGTGTGCGTTG			
	MuEX7-cDNA-FOR	CGGGATACTTGGGAGGAAAATG	RT-PCR	56	RFLP: *Rsa*I
	MuEX9- cDNA-REV	CGTGTGCGTTGATGATGAATGTG			
Hras	Hras-mu-FOR	GACATGTCTACTGGA CATC	RT-PCR	62	SSCP: *Ava*II
	Hras-mu-REV	GATCAACGTGTGCCTCACA			
Nttp1	Nttp1-FOR1	GCTGGACAAGTCCATCGAGT	RT-PCR	62	RFLP: *Sma*I
	Nttp1-FOR2	GGCCTCTCGGCCCTGTCGG	Genomic PCR		
	Nttp1-REV	GAACTCCATCTGGCAGCTGC	Genomic, RT-PCR		

[a]Restriction digestion of the radiolabeled RT-PCR products was used either to score RFLPs or to reduce the size of the SSCP fragments to improve the resolution of the alleles

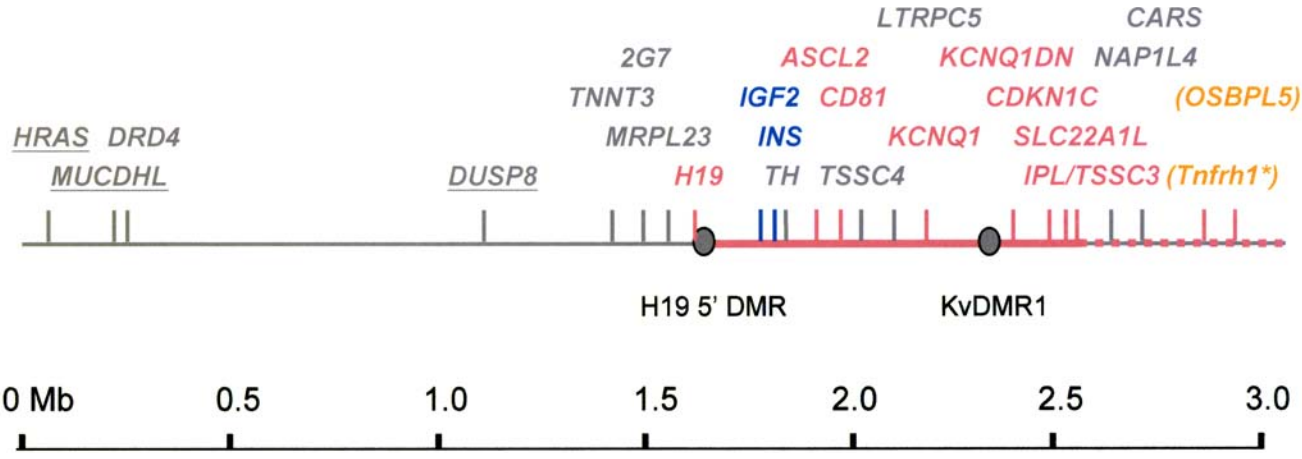

Fig. 1 Map of the imprinted region on human Chr 11p15.5. Genes in *blue* are imprinted and expressed from the paternal allele; genes in *red* are imprinted and expressed from the maternal allele. Assignments are based on combined data from mice and humans. The genes that are the focus of this study are *underlined*. *CD81* is weakly imprinted in yolk sac of mice, and has not been shown imprinted in other tissues. *OSBPL5* (*Obph1*) is indicated in ocher because it is monoallelically expressed only in placenta (Engemann et al. 2000; Higashimoto et al. 2002). The *Tnfrh1* gene is also indicated in *ocher* and marked by an *asterisk*, since it does not appear to have a human orthologue, but it is weakly imprinted in several organs of mice (Clark et al. 2002)

overnight for SSCP; 500 V, 2–3 h for RFLP). For some genes, it was necessary to digest with a restriction enzyme (cutting outside of the polymorphic site) prior to diluting the radiolabeled samples for the SSCP analysis, to reduce the size of the relevant fragments and permit better resolution of the alleles (Table 1). The SSCP and RFLP results were validated by direct sequencing, either with dye-labeled terminators (ABI 377 Sequencer) or by dideoxy termination with ^{35}S-dATP labeling and electrophoresis on 6% denaturing acrylamide gels. Allelic representation in genomic PCR products (Table 1) served as a control for these experiments.

Results

The imprinted region on human Chr 11p15.5 is shown schematically in Fig. 1. Indicated on this map are two DNA elements (DMRs) that show parent-of-origin-dependent differential CpG methylation which are essential for establishing the functional imprints of genes in the two subdomains. The *H19* 5′ DMR controls imprinting of *H19*, *IGF2* and *INS* (*Ins2* in the mouse), while the KvDMR1 element controls imprinting of *KCNQ1*, *ASCL2* (*Mash2*), *SLC22A1L* and *IPL/TSSC3* (Cleary et al. 2001; Fitzpatrick et al. 2002; Horike et al. 2000). Previous data have indicated biallelic expression (lack of imprinting) of several genes downstream of *H19*. This direction is telomeric on human Chr 11p15.5, but centromeric on distal Chr 7 in mice. Genes assessed for allele-specific mRNA expression in multiple tissues include the ribosomal protein gene *MRPL23* (Tsang et al. 1995), the RNA gene *2G7* (Yuan et al. 1996) and the troponin gene *TNNT3* (Yuan et al. 1996). Data from a single post-natal brain sample suggest that the dopamine receptor gene *DRD4*, located 1.5 Mb downstream of *H19*, is also expressed biallelically (Cichon et al. 1996). The *HRAS* and *MUCDHL* genes, which are the main subject of this report, are situated near *DRD4*, close to the Chr 11p15.5 telomere (Goldberg et al. 2002; Paris and Williams 2000).

DNA sequences that are rich in CpG dinucleotides (CpG islands or CpG-rich intragenic sequences) sometimes show allele-specific methylation when they are in or near imprinted genes. A prototype is *H19*, which is densely

Fig. 2a–d DNA methylation at the *MUCDHL* and *H19* loci. Genomic DNAs from WTs, the non-neoplastic kidney parenchyma adjacent to the tumor (*Ki*) and a control fetal kidney (*FKi*) were digested with the indicated restriction enzymes and analyzed by Southern blotting. **a** Blots hybridized with probe A, spanning the CpG-island upstream of *MUCDHL*, which overlaps the small *SCT* gene. This CpG-island is essentially unmethylated in all normal samples, indicated by the absence of protected bands after digestion with the methylation-sensitive restriction enzymes *Hpa*II and *Cfo*I. Faint lower molecular weight bands may represent minor cell populations with partial methylation. Most WTs also show an unmethylated pattern, although two cases (WT39 and WT40) show a partial gain of methylation. The WT cases are numbered as in our previous study (Yeh et al. 2002). WTs 37, 39 and 40 have Chr 11p15.5 LOH, while WT38 retains heterozygosity. **b** Blots stripped and rehybridized with probe B, spanning an internal CpG-rich region of *MUCDHL*. The pattern of partial methylation seen in the WT DNA closely matches that of the control fetal kidney. **c** Blots stripped and rehybridized with probe C, spanning a portion of the *H19* 5′ DMR, which includes several binding sites for the insulator-binding protein CTCF (Bell and Felsenfeld 2000; Frevel et al. 1999; Hark et al. 2000). This probe (*dark bar*) weakly cross-hybridizes with another repeat of this sequence (*light bar*). The biphasic pattern of completely protected bands and smaller unprotected fragments (*vertical bar*), seen in the kidney samples, is characteristic of a DMR associated with an imprinted locus. There is complete methylation in WT37, which has lost the hypomethylated maternal allele via Chr 11p15.5 LOH. *R Rsa*I, *C Cfo*I, *H Hpa*II; restriction maps are shown on the *right*, with *Rsa*I sites indicated by the *tall markings*, and *Cfo*I or *Hpa*II sites by the *short markings*. **d** Methylation mapping of the *MUCDHL* intragenic CpG-rich region by bisulfite-conversion/DNA sequencing in WT34 (with 11p15.5 LOH) and normal adult kidney. The region covered in this analysis is shown by the *double bar* below the map of *MUCDHL* in (B). Each *line* represents one sequenced clone; methylated CpG dinucleotides are indicated by the *filled circles*, and unmethylated CpG dinucleotides by the *open circles*. A heterogeneous pattern of methylation is present in the normal kidney (*Ki*) and in the WT, but there is less overall methylation in the WT. This matches the Southern blot results for this case (not shown)

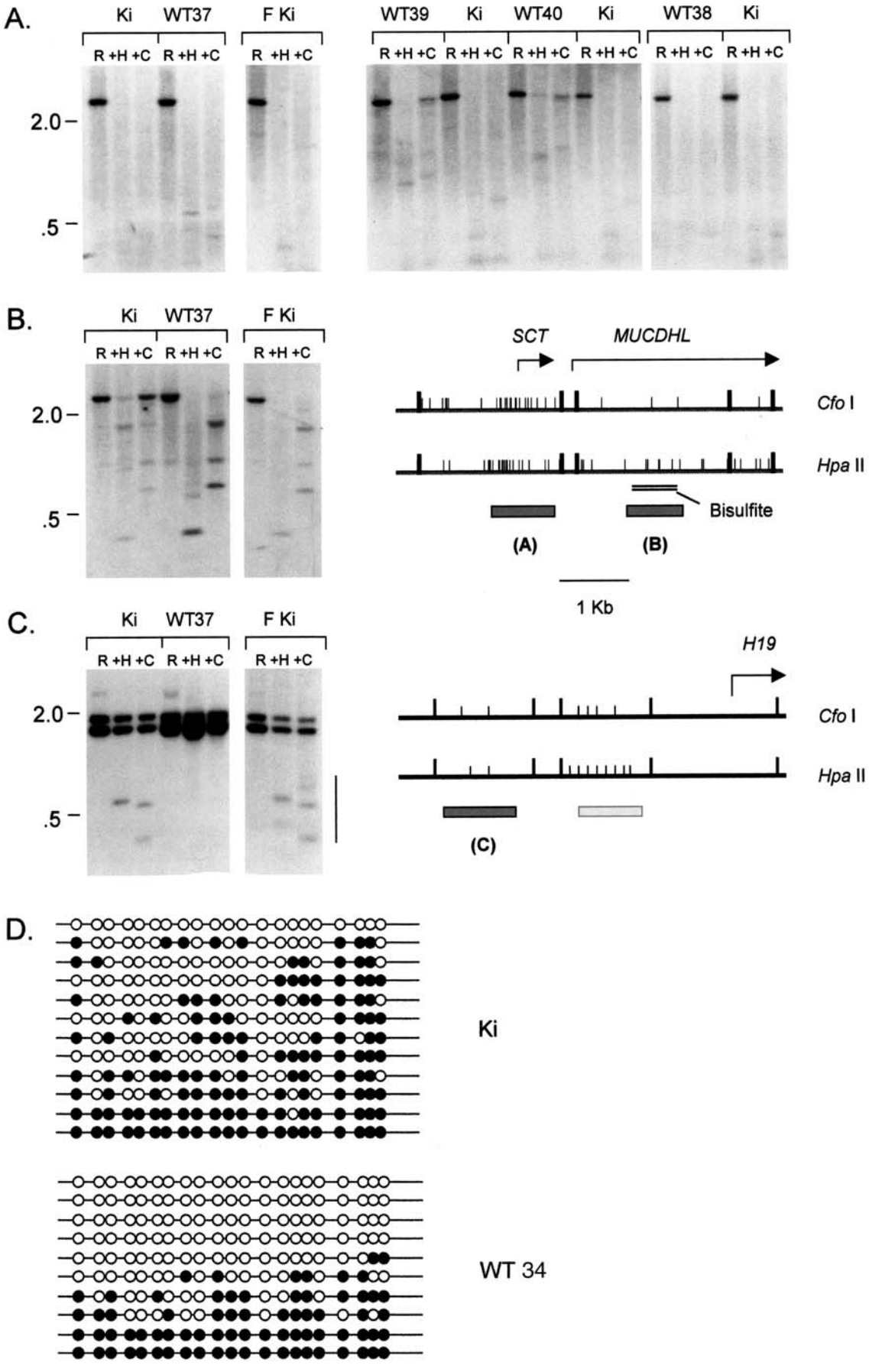
A.
Ki
WT37
F Ki
WT39
Ki
WT40
Ki
WT38
Ki
R +H +C
2.0
.5
B.
SCT
MUCDHL
Cfo I
Hpa II
Bisulfite
(A)
(B)
1 Kb
C.
H19
(C)
D.
Ki
WT 34

methylated, both in the body of the gene and in its upstream sequences, on the silent paternal allele, and not methylated on the transcriptionally active maternal allele (Bartolomei et al. 1993; Zhang et al. 1993). A pathological gain of DNA methylation, correlating with transcriptional silencing, occurs on the maternal allele of *H19* (*H19*^{mat}) in a substantial subset of WTs (Moulton et al. 1994; Taniguchi et al. 1995). Previous studies have suggested that this de novo methylation, sometimes referred to as "loss of imprinting" (LOI) is specific to *H19* and its immediate upstream sequences (Dao et al. 1999), but analysis of additional marker loci is of interest.

The *MUCDHL* gene is preceded at its 5′ end by a classical CpG-island, overlapping the small upstream secretin (*SCT*) gene, and there are CpG-rich areas within the *MUCDHL* transcribed sequences. To determine whether *MUCDHL* shows an "imprinted pattern" of allele-specific DNA methylation, and to ask whether this gene is aberrantly methylated in WTs, we digested DNAs from eight WTs, the associated normal kidney parenchyma of each case, and one normal fetal kidney, with methylation-sensitive restriction enzymes and carried out Southern analysis, hybridizing the blots sequentially with upstream and internal *MUCDHL* probes. As shown for representative samples in Fig. 2a, the upstream CpG-island situated between *SCT* and *MUCDHL* was not detectably methylated in any of the normal samples, and remained hypomethylated in most of the WTs (6/8 cases examined). Two WTs (WT39, WT40) showed partial methylation of this region, but this increased methylation was not correlated with Chr 11p15.5 LOH or LOI. The two cases with partial methylation both showed Chr 11p15.5 LOH, but three other WTs with LOH, two with LOI and one with neither LOH nor LOI did not show a gain of methylation (Fig. 2a, and data not shown). The downstream CpG-rich sequences within the *MUCDHL* gene were partially methylated in both normal and tumor DNAs, with the pattern seen in the WTs closely approximating that of the control fetal kidney (example in Fig. 2b). The heterogeneous pattern of partial CpG methylation in this intragenic region was confirmed at higher resolution by bisulfite-conversion/DNA sequencing (Fig. 2d).

Overall, these findings for *MUCDHL* match the canonical patterns of methylation expected for most (non-imprinted) mammalian genes; i.e., lack of methylation in CpG islands and heterogeneous methylation in CpG-rich intragenic regions (Paulsen and Ferguson-Smith 2001). In contrast, the same Southern blots re-hybridized with a probe for the (imprinted) *H19* 5′ DMR revealed the expected sharply biphasic pattern of methylation in the control kidneys, contrasting with extensive bi-allelic hypermethylation in the WTs with Chr 11p15.5 LOH or LOI (example in Fig. 2c).

To directly assess allele-specific mRNA expression from the human *MUCDHL* gene, we next searched for sequence polymorphisms that would allow the two alleles to be distinguished. Screening the expressed sequence tag (EST) database, followed by direct sequencing of genomic PCR products, revealed two single-nucleotide polymorphisms (SNPs) in *MUCDHL* exons: a A→G change at

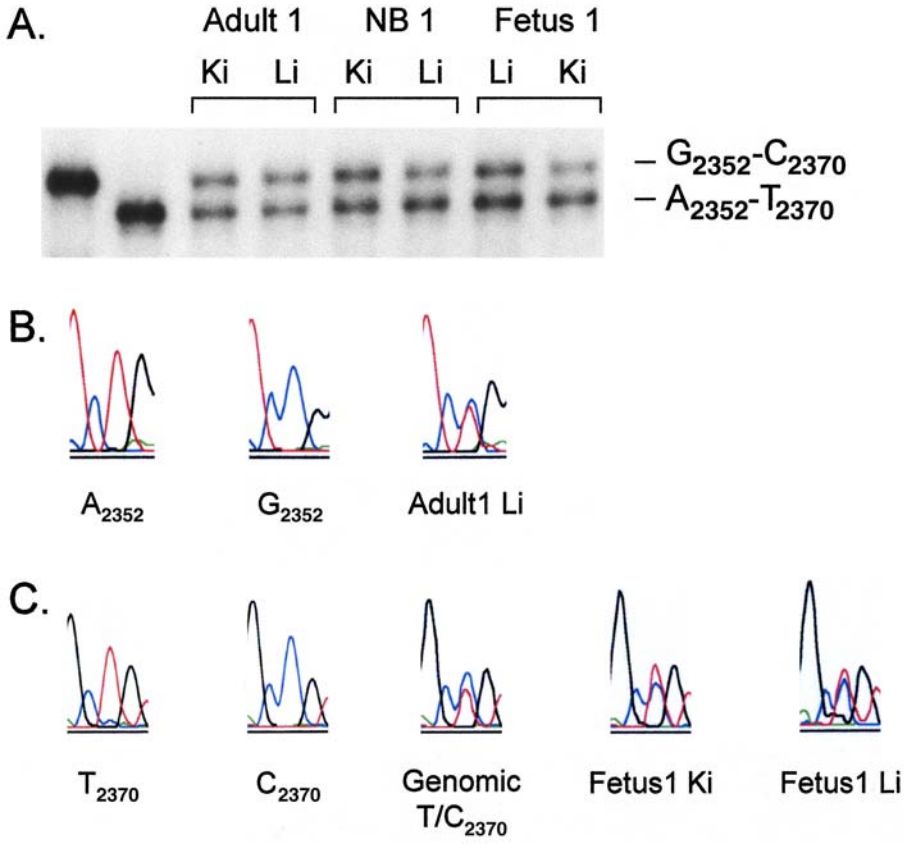

Fig. 3a–c Biallelic expression of the human *MUCDHL* gene. **a** RT-PCR/SSCP analysis of samples from individuals heterozygous for both SNPs. The haplotypes corresponding to each allele are indicated *on the right*. The two lanes *on the left* are from individuals homozygous for each haplotype. **b** Confirmation of biallelic expression in the liver of adult 1 by direct sequencing of the RT-PCR product through the 2352A/G SNP. Sequencing chromatograms from the two homozygotes are shown for comparison. **c** Confirmation of biallelic expression in the kidney and liver of fetus 1 by direct sequencing through the 2370T/C SNP (*Ki* kidney, *Li* liver)

position 2352 and a T→C change at position 2370 (the sequence for the *MUCDHL* mRNA is GenBank accession no. AF301909). From 20 individuals autopsied at various developmental stages, we identified six who were heterozygous for one or both markers: one mid-gestation fetus, three newborns, one four-year-old child, and one adult. As illustrated for several cases in Fig. 3a, SSCP analysis indicated biallelic representation in all RT-PCR products, although there were minor variations in the intensities of the allele-specific bands. Biallelic expression was confirmed in each case by direct sequencing of the PCR products (Fig. 3b, and data not shown).

Crossing divergent mouse strains and analyzing allele-specific RNA expression in the F1 conceptuses is a standard test for imprinting. Screening of the mouse *Mucdhl* sequences in genomic and cDNA PCR products revealed a SNP, an A→G change at position 822 of the reference mRNA sequence (GenBank accession no. AK007988), that distinguished the *Mus musculus domesticus*-derived laboratory strain C57BL/6 from *Mus musculus castaneus* (CAST). This SNP created an *Rsa*I RFLP. In multiple fetal and adult tissues from interspecific crosses, there was equal biallelic expression of *Mucdhl* (Fig. 4a). Importantly, the relative intensities of the two alleles did not vary according to the "direction" of the crosses: identical results were obtained regardless of whether the mother was CAST or C57BL/6 (Fig. 4a). That the RFLP analysis was giving a linear readout of allelic expression was verified by mixing known amounts of pure CAST and C57Bl/6 templates prior to radiolabeling and RFLP analysis (Fig. 4b). The data were further validated by direct sequencing of the cDNA PCR products, which confirmed equal biallelic expression, independent of the parent-of-origin of the alleles (Fig. 4c).

The *HRAS* gene is situated slightly telomeric to *MUCDHL* (Fig. 1). The mouse orthologue, *Hras*, shows conserved linkage with the other genes in the imprinted region of mouse distal Chr 7 (although there is an inversion of the entire block of genes in the mouse, relative to the human). In unpublished data that we cited in a previous report (Dao et al. 1999), we tested for possible imprinting of *Hras* in interspecific mouse crosses, and found equal biallelic expression in multiple tissues. These data, which were obtained by SSCP analysis of RT-PCR products spanning an exonic SNP, are shown here in Fig. 5a. These data were confirmed by direct sequencing (Fig. 5b). In that experiment, we examined an additional locus, the mouse *Nttp1* gene, which is the orthologue of human *DUSP8*, and which is located between *H19* and *Hras* (Fig. 1). Using a similar approach of RT-PCR and SSCP analysis, this gene too was found equally expressed from the two parental alleles in multiple organs from F1 progeny of interspecific mouse crosses. Tissues and stages examined were brain, whole fetus, liver, heart, extraembryonic membranes, and placenta from reciprocal (BL/6 × CAST) and (CAST × BL/6) crosses at 12.5 dpc (Fig. 5c), and these same organs and tissues, as well as lung and ribs from 14.5 dpc conceptuses (data not shown).

Failure to find common exonic polymorphisms has thus far prevented us from analyzing human *DUSP8*. However, we identified a frequent exonic polymorphism in the human *HRAS* gene (a T→C substitution at position 81 of the *HRAS* mRNA sequence, GenBank accession no. NM_005343) and utilized RT-PCR across the region con-

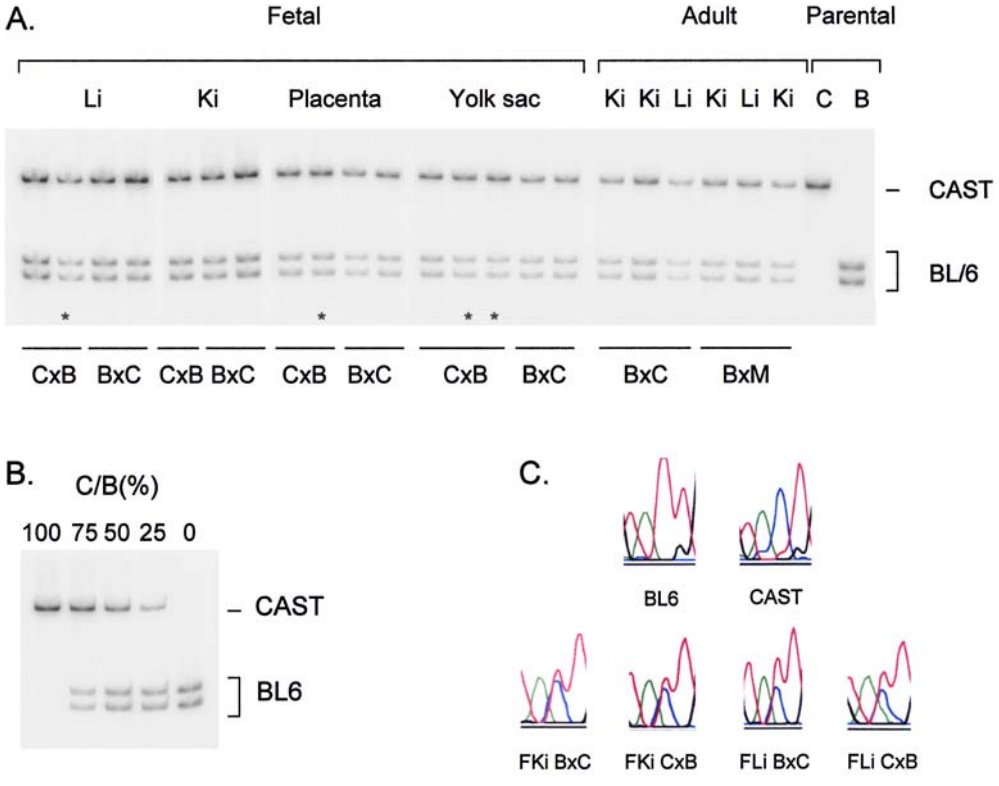

Fig. 4a–c Biallelic expression of *Mucdhl* in fetal and adult organs from (F1) interspecific mouse crosses. **a** RFLP analysis of RT-PCR products. Some samples were analyzed in duplicate to show the reliability of the analysis. Most of the fetal-stage samples were obtained at 14.5 days post-coitum (dpc); the *asterisks* indicate samples obtained at 12.5 dpc. **b** Template mixing experiment showing linearity of the RFLP assay. **c** Confirmation of the RT-PCR/RFLP data by direct sequencing of the RT-PCR products. Chromatograms from the products generated from parental strains (kidney cDNAs) and from the indicated organs of the F1 progeny are indicated. The directions of the crosses are indicated in the conventional manner (maternal × paternal) (*C* CAST, *B* BL/6, *Ki* kidney, *Li* liver)

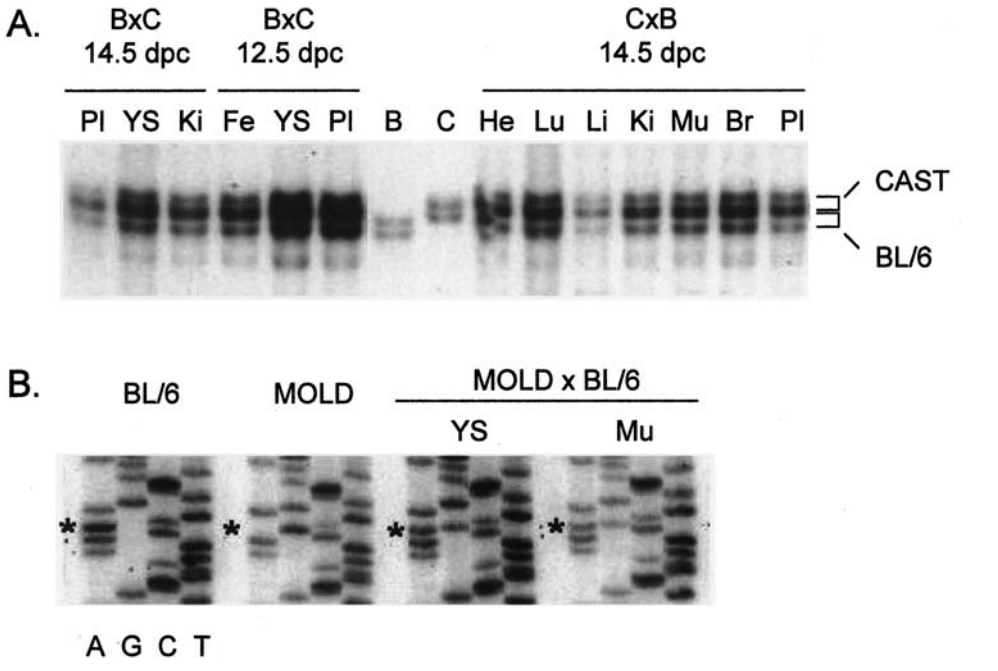

Fig. 5a–c Biallelic expression of *Hras* and *Nttp1* in mice. **a** SSCP analysis showing biallelic expression of *Hras* in fetal tissues from interspecific mouse crosses. Each allele is resolved as a doublet. **b** Confirmation of biallelic expression of *Hras* in yolk sac and muscle by direct sequencing. *Asterisks* mark the SNP distinguishing the two alleles, an A→G change at position 474 of *Hras* mRNA, GenBank accession no. NM_008284, present in both CAST and in another divergent strain, *Mus musculus mollosinus* (*MOLD*). **c** Analysis of allele-specific expression of the *Nttp1* gene. RT-PCR generated a product containing an exonic *Sma*I RFLP (a C→T change at position 1,613 of the *Nttp1* mRNA, GenBank accession no. X95518). There is equal representation of both alleles in yolk sac, brain and placenta, and in whole fetus at 12.5 dpc. Similar data were obtained at 14.5 dpc (not shown). The results from genomic PCR are shown as a control (*C* CAST, *B* BL/6, *Pl* placenta, *YS* yolk sac, *Ki* kidney, *Fe* fetus, *Lu* lung, *Li* liver, *Mu* limb muscle, *Br* brain)

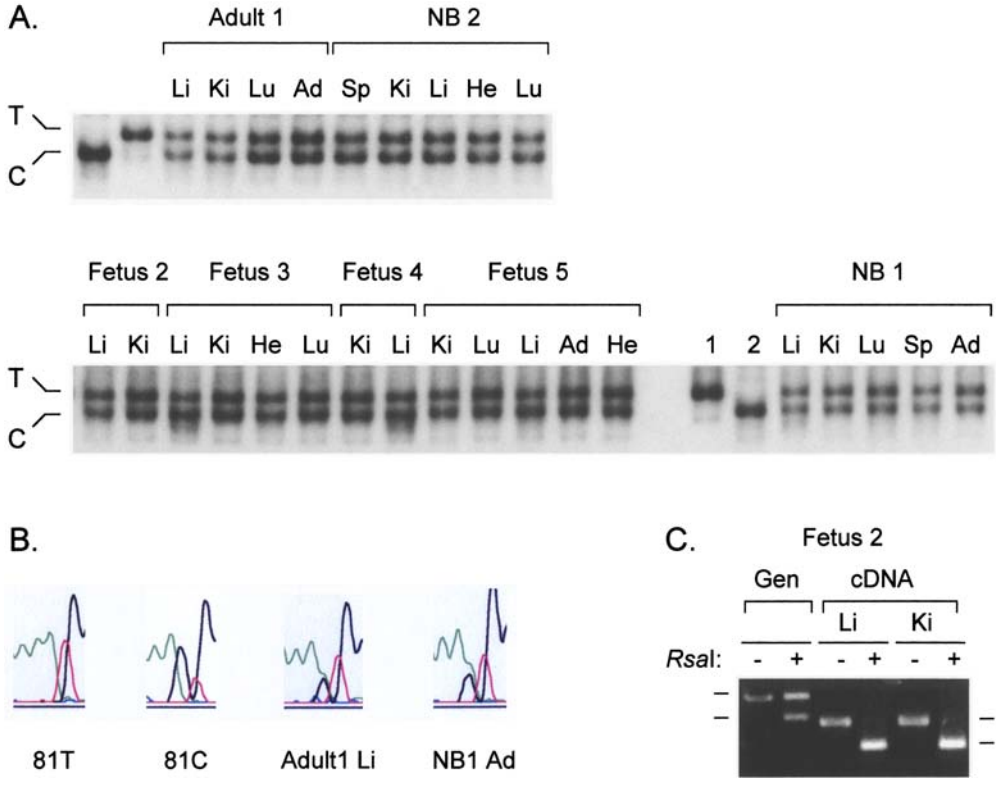

Fig. 6a–c Biallelic expression of human *HRAS*. **a** SSCP analysis showing equal expression of the two *HRAS* alleles in fetuses, newborns and an adult. *Lanes 1, 2* contain RT-PCR products from homozygotes. **b** Confirmation of the SSCP data by direct sequencing of RT-PCR products through the *HRAS* SNP. Sequences from two homozygotes and two heterozygotes are shown. Sequences were obtained with the reverse primer. **c** Monoallelic expression of the imprinted gene *H19* in the same tissue samples. Results for the *H19 Rsa*I RFLP (Zhang and Tycko 1992) in one of the fetuses are shown. There is biallelic representation in the genomic PCR product (two bands in the *lane* +*Rsa*I), and virtually monoallelic representation in the RT-PCR product (single band in *lanes* +*Rsa*I). The small fragment produced by *Rsa*I digestion is at a much lower position on the gel and is not shown. The size of the RT-PCR product is smaller than the genomic PCR product, due to RNA splicing (*Ki* kidney, *Lu* lung, *Li* liver, *Ad* adrenal, *He* heart, *Sp* spleen, *Gen* genomic PCR)

taining this SNP, followed by SSCP analysis, to examine allele-specific expression in multiple organs. As shown in Fig. 6a, liver, kidney, lung, adrenal and heart from each of three developmental stages (mid-gestation fetus, newborn and adult) showed equal biallelic expression of *HRAS*. These results were confirmed by direct sequencing (Fig. 6b). As an additional control, we amplified the same single-stranded cDNA preparations using PCR primers for the *H19* gene, and found the expected pattern of monoallelic expression, as indicated by RFLP analysis (Fig. 6c).

Discussion

Based on these results, combined with previous data, at least seven genes in 1.5 Mb of DNA downstream of *H19*, namely *HRAS*, *MUCDHL*, *DRD4*, *DUSP8*, *TNNT3*, *2G7*, and *MRPL23*, are biallelically expressed in one or more organs of humans and/or mice. Since functional imprinting can be exquisitely tissue-specific (for example, Rougeulle et al. 1997), it is not possible to definitively exclude imprinting by examining a finite set of tissues. But given this caveat, the current data strengthen the conclusion that the imprinted region on Chr 11p15.5 has a definite border, with a substantial length of sub-telomeric DNA intervening between the telomere and the *H19* gene, at the beginning of the imprinted region. This is consistent with the notion that imprinting is dictated not by chromosomal position per se, but rather by *cis*-acting elements that are intrinsic to the DNA sequences in and around imprinted genes, which have a limited range of action. Experimental data supporting this model have come from studies of transgenic mice carrying large-insert (YAC, BAC) transgenes spanning imprinted genes. In some instances, including experiments with transgenes spanning *H19*, the transgenic constructs have faithfully recapitulated the imprinting of the corresponding endogenous loci, independently of chromosomal integration sites (Ainscough et al. 1997).

While *H19* marks one border of the imprinted region, the other border, which must exist centromeric (in humans) of the strongly imprinted *IPL* (*TSSC3*) gene, is less well defined. We recently documented weak but consistent imprinting of the *Tnfrh1* gene in mice (Clark et al. 2002), suggesting that the influence of the imprinting center defined by KvDMR1 extends for a considerable distance. In contrast to all other genes in this region, *Tnfrh1* does not seem to have a human orthologue. The *NAP1L4* gene is expressed biallelically in humans (Hu et al. 1996), and the *Cars* gene is biallelically expressed in mice (Engemann et al. 2000). The *Osbph1* gene is expressed biallelically in all mouse tissues except placenta (Engemann et al. 2000). Monoallelic expression from the maternal allele observed in placenta might reflect either imprinting or expression from maternal cells, but a recent report of an allelic bias in placenta at 8.5 days post-coitum (a stage at which there is minimal maternal contamination) supports imprinting (Higashimoto et al. 2002). More data will be needed to define the position of this border of the imprinted region. A more perplexing problem is raised by the bipartite structure of the imprinted region. It remains unclear whether the close apposition of the two imprinted sub-domains is simply a coincidence or alternatively has some unifying mechanistic basis.

Lastly, what is the biological significance of lack of imprinting of *MUCDHL* and *HRAS*? *HRAS* is a well-studied proto-oncogene, and Ras proteins normally function in intracellular signaling downstream of plasma membrane receptors. Since the phenotype of homozygous *Hras*$^{-/-}$ knockout mice is unexpectedly mild (viable and fertile without developmental anomalies), a detailed examination of the heterozygotes has not been undertaken (Esteban et al. 2001). Our data showing lack of imprinting of *Hras* predict that, if a phenotype can be found due to deletion of this gene, it will segregate in a Mendelian fashion.

Mu-protocadherin, encoded by the *MUCDHL* gene, is a developmentally regulated cell adhesion molecule that is expressed in various epithelial tissues (Goldberg et al. 2000). This protein, which is composed of multiple cadherin ectodomains, as well as multiple mucin repeats in its longer isoform, is displayed on the apical surface of differentiated proximal tubule epithelial cells of the kidney, where it may have additional functions unrelated to adhesion (Goldberg et al. 2002). In principle, cell adhesion molecules are candidate tumor suppressors, as exemplified by E-cadherin, which is silenced and/or mutated in human breast and gastric cancers (Guilford et al. 1998; Hajra and Fearon 2002). While our current data, indicating minor and infrequent epigenetic modification of the *MUCDHL* gene in WTs, do not suggest a tumor suppressor role for mu-protocadherin, future studies of the expression and CpG-methylation of this gene in adult kidney neoplasms will be of some interest.

Acknowledgements This work was supported by grant R01 CA60765 from the N.I.H. to B.T., and by grants from the March of Dimes and the Spunk Fund, Inc. to M.G..

References

Ainscough JF, Koide T, Tada M, Barton S, Surani MA (1997) Imprinting of *Igf2* and *H19* from a 130 kb YAC transgene. Development 124:3621–3632

Bartolomei MS, Webber AL, Brunkow ME, Tilghman SM (1993) Epigenetic mechanisms underlying the imprinting of the mouse *H19* gene. Genes Dev 7:1663–1673

Bell AC, Felsenfeld G (2000) Methylation of a CTCF-dependent boundary controls imprinted expression of the *Igf2* gene. Nature 405:482–485

Brannan CI, Bartolomei MS (1999) Mechanisms of genomic imprinting. Curr Opin Genet Dev 9:164–170

Cichon S, Nothen MM, Wolf HK, Propping P (1996) Lack of imprinting of the human dopamine D4 receptor (*DRD4*) gene. Am J Med Genet 67:229–231

Clark L, Wei M, Cattoretti G, Mendelsohn C, Tycko B (2002) The *Tnfrh1* (*Tnfrsf23*) gene is weakly imprinted in several organs and expressed at the trophoblast-decidua interface. BMC Genet 3:11

Cleary MA, van Raamsdonk CD, Levorse J, Zheng B, Bradley A, Tilghman SM (2001) Disruption of an imprinted gene cluster by a targeted chromosomal translocation in mice. Nat Genet 29:78–82

Dao D, Walsh CP, Yuan L, Gorelov D, Feng L, Hensle T, Nisen P, Yamashiro DJ, Bestor TH, Tycko B (1999) Multipoint analysis of human chromosome 11p15/mouse distal chromosome 7: inclusion of *H19*/*IGF2* in the minimal WT2 region, gene specificity of *H19* silencing in Wilms' tumorigenesis and methylation hyper-dependence of *H19* imprinting. Hum Mol Genet 8:1337–1352

Engemann S, Strodicke M, Paulsen M, Franck O, Reinhardt R, Lane N, Reik W, Walter J (2000) Sequence and functional comparison in the Beckwith-Wiedemann region: implications for a novel imprinting centre and extended imprinting. Hum Mol Genet 9:2691–2706

Esteban LM, Vicario-Abejon C, Fernandez-Salguero P, Fernandez-Medarde A, Swaminathan N, Yienger K, Lopez E, Malumbres M, McKay R, Ward JM, Pellicer A, Santos E (2001) Targeted genomic disruption of *H-ras* and *N-ras*, individually or in combination, reveals the dispensability of both loci for mouse growth and development. Mol Cell Biol 21:1444–1452

Feinberg AP (2000) The two-domain hypothesis in Beckwith-Wiedemann syndrome. J Clin Invest 106:739–740

Fitzpatrick GV, Soloway PD, Higgins MJ (2002) Regional loss of imprinting and growth deficiency in mice with a targeted deletion of KvDMR1. Nat Genet (in press)

Frevel MA, Sowerby SJ, Petersen GB, Reeve AE (1999) Methylation sequencing analysis refines the region of *H19* epimutation in Wilms tumor. J Biol Chem 274:29331–29340

Goldberg M, Peshkovsky C, Shifteh A, Al-Awqati Q (2000) mu-Protocadherin, a novel developmentally regulated protocadherin with mucin-like domains. J Biol Chem 275:24622–24629

Goldberg M, Wei M, Tycko B, Falikovich I, Warburton D (2002) Identification and expression analysis of the human mu-protocadherin gene in fetal and adult kidneys. Am J Physiol (in press)

Guilford P, Hopkins J, Harraway J, McLeod M, McLeod N, Harawira P, Taite H, Scoular R, Miller A, Reeve AE (1998) E-cadherin germline mutations in familial gastric cancer. Nature 392:402–405

Hajra KM, Fearon ER (2002) Cadherin and catenin alterations in human cancer. Genes Chromosomes Cancer 34: 255–268

Hark AT, Schoenherr CJ, Katz DJ, Ingram RS, Levorse JM, Tilghman SM (2000) CTCF mediates methylation-sensitive enhancer-blocking activity at the *H19*/*Igf2* locus. Nature 405: 486–489

Herman JG, Graff JR, Myohanen S, Nelkin BD, Baylin SB (1996) Methylation-specific PCR: a novel PCR assay for methylation status of CpG islands. Proc Natl Acad Sci USA 93:9821–9826

Higashimoto K, Soejima H, Yatsuki H, Joh K, Uchiyama M, Obata Y, Ono R, Wang Y, Xin Z, Zhu X, Masuko S, Ishino F, Hatada I, Jinno Y, Iwasaka T, Katsuki T, Mukai T (2002) Characterization and Imprinting Status of OBPH1/Obph1 Gene: Implications for an Extended Imprinting Domain in Human and Mouse. Genomics 80:575–584

Horike S, Mitsuya K, Meguro M, Kotobuki N, Kashiwagi A, Notsu T, Schulz TC, Shirayoshi Y, Oshimura M (2000) Targeted disruption of the human *LIT1* locus defines a putative imprinting control element playing an essential role in Beckwith-Wiedemann syndrome. Hum Mol Genet 9:2075–2083

Hu RJ, Lee MP, Johnson LA, Feinberg AP (1996) A novel human homologue of yeast nucleosome assembly protein, 65 kb centromeric to the p57KIP2 gene, is biallelically expressed in fetal and adult tissues. Hum Mol Genet 5:1743–1748

Maher ER, Reik W (2000) Beckwith-Wiedemann syndrome: imprinting in clusters revisited. J Clin Invest 105:247–252

Moulton T, Crenshaw T, Hao Y, Moosikasuwan J, Lin N, Dembitzer F, Hensle T, Weiss L, McMorrow L, Loew T, et al. (1994) Epigenetic lesions at the *H19* locus in Wilms' tumour patients. Nat Genet 7:440–447

Nicholls RD (2000) The impact of genomic imprinting for neurobehavioral and developmental disorders. J Clin Invest 105: 413–418

Orita M, Iwahana H, Kanazawa H, Hayashi K, Sekiya T (1989) Detection of polymorphisms of human DNA by gel electrophoresis as single-strand conformation polymorphisms. Proc Natl Acad Sci USA 86:2766–2770

Paris MJ, Williams BR (2000) Characterization of a 500-kb contig spanning the region between *c-Ha-Ras* and *MUC2* on chromosome 11p15.5. Genomics 69:196–202

Paulsen M, Ferguson-Smith AC (2001) DNA methylation in genomic imprinting, development, and disease. J Pathol 195:97–110

Rougeulle C, Glatt H, Lalande M (1997) The Angelman syndrome candidate gene, *UBE3A*/*E6-AP*, is imprinted in brain. Nat Genet 17:14–15

Taniguchi T, Sullivan MJ, Ogawa O, Reeve AE (1995) Epigenetic changes encompassing the IGF2/H19 locus associated with relaxation of *IGF2* imprinting and silencing of *H19* in Wilms tumor. Proc Natl Acad Sci USA 92:2159–2163

Tsang P, Gilles F, Yuan L, Kuo YH, Lupu F, Samara G, Moosikasuwan J, Goye A, Zelenetz AD, Selleri L, et al. (1995) A novel *L23*-related gene 40 kb downstream of the imprinted *H19* gene is biallelically expressed in mid-fetal and adult human tissues. Hum Mol Genet 4:1499–507

Tycko B (2000) Epigenetic gene silencing in cancer. J Clin Invest 105:401–407

Tycko B, Morison IM (2002) Physiological functions of imprinted genes. J Cell Physiol 192:1-15

Yeh A, Wei M, Golub SB, Yamashiro DJ, Murty VV, Tycko B (2002) Chromosome arm 16q in Wilms tumors: unbalanced chromosomal translocations, loss of heterozygosity, and assessment of the *CTCF* gene. Genes Chromosomes Cancer 35: 156–163

Yuan L, Qian N, Tycko B (1996) An extended region of biallelic gene expression and rodent-human synteny downstream of the imprinted *H19* gene on chromosome 11p15.5. Hum Mol Genet 5:1931–1937

Zhang Y, Tycko B (1992) Monoallelic expression of the human *H19* gene. Nat Genet 1:40-44

Zhang Y, Shields T, Crenshaw T, Hao Y, Moulton T, Tycko B (1993) Imprinting of human *H19*: allele-specific CpG methylation, loss of the active allele in Wilms tumor, and potential for somatic allele switching. Am J Hum Genet 53:113–124